

**Joanna SULEJ-CHOJNACKA^{*}, Agnieszka WIELOWIEJSKA-
-GIERTUGA^{*}, Adrian MRÓZ^{*}, Daniel DELFOSSE^{**}**

FRETTING CORROSION OF COBALT AND TITANIUM IMPLANT ALLOYS IN SIMULATED BODY FLUIDS

BADANIA FRETTING-KOROZJI IMPLANTACYJNYCH STOPÓW KOBALTU I TYTANU W ŚRODOWISKU SUROWICY BYDŁĘCEJ

Key words:

fretting corrosion, biomaterials, CoCrMo alloy, Ti6Al4V alloy, endoprosthesis

Słowa kluczowe:

fretting-korozja, biomateriały, stop CoCrMo, stop Ti6Al4V, endoproteza

Abstract

The most important advantage of using modular hip joint endoprostheses is the possibility to adapt the endoprosthesis to the morphology and size of individual patients. However, the additional contact surface is subjected to fretting wear due to mutual micro displacements and the aggressive chemistry of the environment inside the human body (fretting corrosion).

^{*} Metal Forming Institute, al. Jana Pawła II 14, 61-139 Poznań, Poland, tel. +48 61 657 05 55, e-mail: joanna.chojnacka@inop.poznan.pl.

^{**} Mathys Ltd Bettlach (Switzerland).

Today's hip endoprotheses are generally composed of a hip stem, a femoral ball head and an acetabular cup (**Figure 1**). The hip stem is made of stainless steel, CoCrMo or a Ti alloys. The femoral ball head is made of stainless steel, CoCrMo, or a ceramic material. In the case of a modular hip stem, i.e. with a modular neck portion, the materials used are generally CoCrMo and Ti6Al 4V. (The interface between femoral ball head and the acetabular cup is an articulating surface and not the subject of this research project.)

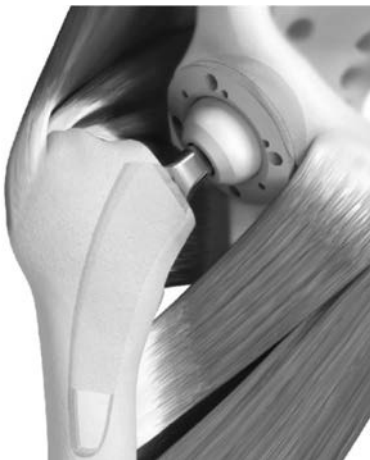


Fig. 1. Modern modular hip endoprotheses with hip stem, femoral ball head and acetabular cup (here: optimys stem, ceramys head and RM Pressfit vitamys cup by Mathys Ltd. Bettlach)

Rys. 1. Współczesna endoproteza stawu biodrowego z trzpieniem, głową oraz panewką (na zdjęciu: trzpień optimys[®], ceramiczna głowa oraz polimerowa panewka RM Pressfit firmy Mathys Ltd. Bettlach)

In this framework, a comparative study of the fretting corrosion resistance of the three most common metallic material combinations occurring in a modular, the non-articulating connection of total hip joint endoprotheses (CoCrMo-CoCrMo, CoCrMo-Ti6Al4V, and Ti6Al4V-Ti6Al4V) was undertaken. Studies were performed with a tribological tester, working in articulating-reciprocating motion, integrated with a potentiostat equipped with a tri-electrode system. The tribosystem consisted of a fixed stem pressed with a constant force to a plate performing the reciprocating motion of a predetermined frequency and amplitude. The tests were performed in diluted bovine serum at 37°C.

Based on the obtained results, it was found that the greatest resistance to corrosion in static conditions was exhibited by the CoCrMo-CoCrMo friction pair, while the lowest ΔE value was obtained by CoCrMo-Ti6Al4V. It also

confirmed the existence of a correlation between the intensity of the depassivation process caused by the mechanical destruction of the surface layer and the friction resistance values in the tribological system.

INTRODUCTION

Most of the currently used total hip endoprostheses are characterized by the presence of at least one modular connection. The most common combination in a modular total hip endoprosthesis is a head-stem neck junction. The endoprostheses currently applied not only differ from each other in construction, but also regarding the applied materials [L. 2]. The use of such a design solution provides certain advantages. The most important is the ability to make an intra-operative decision regarding the size of the head that is best suited for the individual patient. In addition, this provides the possibility of leaving the stem in-situ in a revision case by only exchanging the bearing components, which is the head and the acetabular cup or inlay [L. 1]. Unfortunately, this solution also has some drawbacks; each additional modular connection is an area subjected to mutual micro displacements and time-varying load values [L. 3].

Metal alloys that are used in endoprosthesis elements owe their corrosion resistance in the environment of bodily fluids to their ability to form a stable passivation layer on the surface. Due to the mutual displacement of metal surfaces, these layers may be subject to cyclic mechanical destruction. In combination with the aggressive action of the biological environment, this leads to degradation of the material in a process called “tribocorrosion.” As a result, wear particles are generated and ions of the metal alloy are released into the human body. This may result in a biological response of the organism. Tribocorrosion of endoprosthesis components can also lead to the development of intergranular corrosion, crack propagation, and catastrophic component failure [L. 4].

The destruction process of implant components results in a reduction of their service life and adversely affects the patients' quality of life. A particular issue that has been underexplored is the process of the destruction of the components of modular endoprostheses due to fretting corrosion. Fretting is defined as a process of relative oscillatory micro-displacements of the contacting surfaces, which result in the destruction of the surface layers of elements coming into contact [L. 5, 6]. In order to distinguish fretting from other wear mechanisms, the authors of article [L. 7] proposed the following equation:

$$e = \frac{D}{a} \quad (1)$$

Fretting is defined as a situation where factor e , the ratio of relative displacement (D) to the width of the contact surface in the direction of displacement (a), is less than 1. If the process takes place in a chemically aggressive environment, i.e. when the passive layer is reconstructed on the interface between the two materials in contact, then we are dealing with fretting corrosion.

One way to study fretting corrosion is to use a tribological tester with an integrated potentiostat equipped with a tri-electrode system [L. 7, 8]. These studies allow the evaluation of the relative fretting corrosion resistance of the tested materials. Factors that affect the obtained test results include contact geometry, surface roughness, displacements range, motion frequency, the load system, and the type of lubricant and temperature [L. 9]. Therefore, the fact that a uniform standard defining testing methodology and values of the parameters mentioned above has not yet been proposed, the possibility of comparing the results available from literature is limited. As part of this work, actions have been taken to propose a fretting corrosion test methodology and to compare the fretting corrosion resistance of three of the most common material combinations used in head-stem neck modular junctions in total hip joint endoprostheses.

TESTING METHODOLOGY

The schematics of the fretting corrosion testing station are shown in **Figure 2**. The station consists of a T-17 tribological tester (ITeE Radom) used to determine the tribological characteristics of the material combinations in an articulating-reciprocating motion [L. 2], which is connected to an SP-150 potentiostat (Bio-Logic Science Instruments) with a low current adapter with a set of electrodes. The tested electrode (“working electrode”) consists of a plate of the tested biomaterial with a surface area of 1 cm^2 . A saturated calomel electrode (SCE) is applied as the reference electrode, and the current electrode is a platinum electrode.

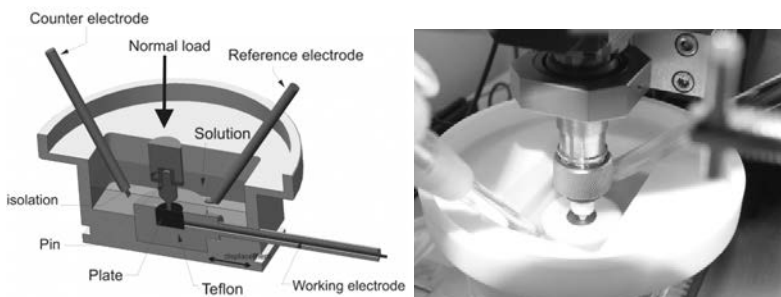


Fig. 2. Schematic of the test equipment for fretting-corrosion testing (T-17 tribometer and SP-150 potentiostat)

Rys. 2. Schemat układu do badania frettingu-korozji (tester tribologiczny T-17 i potencjostat SP-150)

The tribosystem of the fretting corrosion test consisted of a fixed stem pressed with the constant force of 100 N to a plate with dimensions $\text{Ø}14 \times 10$ mm carrying out reciprocating motion at a frequency of 1 Hz with a stroke length of 400 μm . The tests were performed in an aqueous solution of bovine serum with a protein concentration of 25 g/l containing 0.2% sodium azide and EDTA (7.45 g/l). In order to isolate the individual elements of the tribosystem, the measuring cell was made of Teflon and the stem was placed in a special housing made of a non-conductive material.

The following material combinations were subject of testing: CoCrMo-CoCrMo (ISO 5832-12: 2007), Ti6Al4V-Ti6Al4V (ISO 5832-3: 1996), and CoCrMo-Ti6Al4V. Before testing, the friction surfaces were subjected to polishing to obtain a roughness of $R_a = 0.4 \mu\text{m}$. This value corresponds to the surface roughness of modular head-neck stem junction components of commercially available endoprostheses. Before testing, the samples were washed in an ultrasonic cleaner in ethanol (10 min), and distilled water (10 min) and then thoroughly dried.

Each test was divided into three phases. In the first phase (stabilisation for 5400 s), the unloaded sample was immersed in the fluid lubricant under static conditions, i.e. without displacements of the pin with respect to the plate. In the second phase (fretting corrosion for 3600 s), the tribosystem was loaded and subjected to fretting. In the third phase, repassivation was allowed for 3600 s. All trials were performed in triplicate.

The friction surface roughness measurements were performed using a T8000 profilometer (Hommel) with a TKU300 measuring tip. In order to confirm that the process of fretting during the course of the conducted work takes place (condition described by equation (1)), measurement of the width of wear scar was performed using an ECLIPSE L150 optical microscope.

TEST RESULTS AND THEIR ANALYSIS

The resulting wear scar obtained after fretting corrosion testing on a disc made of a cobalt alloy is shown in **Figure 3**.

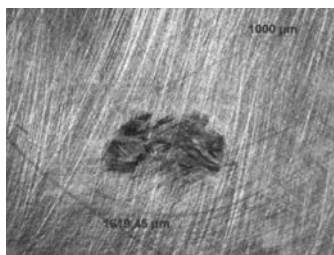


Fig. 3. Image of wear scar after fretting corrosion of CoCrMo alloy

Rys. 3. Obraz morfologii powierzchni po procesie fettegu otrzymany na stopie CoCrMo

The microscopic observation of the surface is a clear confirmation that an intensive process of fretting wear has occurred. Poor removal of wear products from the friction zone is characteristic of fretting processes [L. 4], and a high wear debris concentration is observed at the edges of the wear area.

Figure 4 shows the change of the open circuit potential (OCP) values for the investigated fretting pairs. After the stabilization phase at 5400 s, the fretting friction process was started and led to immediate destruction of the protective passive layer and rapid reduction in the OCP value. During the fretting phase, the friction region behaves as an anode and the counter specimen surface as a cathode [L. 10]. As soon as the motion is initiated, cracking and destruction of the oxide layer occurs. The metal surface is not passivated at the same rate as it is destroyed, because the lubricant restricts the access to oxygen and strongly reacts with the electrolyte.

The observed fluctuations of the OCP value in the fretting phase of the test are due to periodic removal (depassivation) and reconstruction (repassivation) of the passive oxide layer. These fluctuations are the result of a dynamic equilibrium between the depassivation and repassivation processes [L. 11].

After termination of the friction process, the oxide layer is reconstructed in the repassivation phase, resulting in an increase of the OPC values. The ideal situation would be if the OPC value would rapidly reach a constant value equal to the initial value (i.e. the OCP potential value before the fretting process).

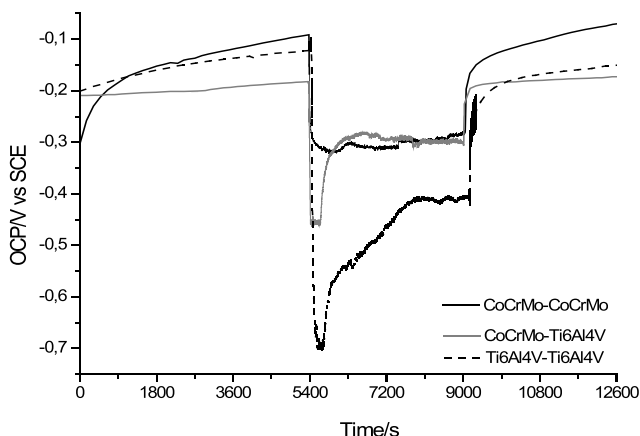


Fig. 4. Changes of the OCP value for the investigated friction pairs

Rys. 4. Zmiany wartości potencjału obwodu otwartego dla badanych par trących

The two pairings CoCrMo-CoCrMo and CoCrMo-Ti6Al4V reach the initial OCP values again within a short time during the repassivation phase. However, for the Ti6Al4V-Ti6Al4V pair, a definite decrease in the OCP value after

completion of the third phase is observed when compared to the first phase. This shows that the oxide layer for this pair does not rebuild completely and leads to lower OCP values, which is also noted in the study by the authors of [L. 12].

From the obtained data, the drop in the value of potential ΔE and the average potential value during the fretting phase E_{avg} was determined. The obtained results are summarized in **Table 1**.

Table 1. Summary of ΔE and E_{avg} of open circuit potential values for the investigated friction pairs

Tabela 1. Zestawienie ΔE oraz E_{avg} wartości potencjału obwodu otwartego dla badanych par trących otrzymanych w wyniku mechanicznej depasywacji spowodowanej frettingiem

Material combination (stem-plate)	ΔE	E_{avg} [V]
CoCrMo-CoCrMo	0.21009	-0.3014
CoCrMo-Ti6Al4V	0.12384	-0.3052
Ti6Al4V-Ti6Al4V	0.39061	-0.4843

When analysing the data presented in **Fig. 3** and **Table 1**, it can be concluded that the best corrosion resistance under static conditions is exhibited by the CoCrMo-CoCrMo friction pair for which the highest OCP value was obtained. In contrast, the lowest ΔE value was measured for the pair in which the stem was made of CoCrMo alloy and the plate of Ti6Al4V alloy. The interactions between the CoCrMo and Ti6Al4V surfaces are not exactly known. It is evident that the oxide mechanical and electrochemical interactions depend on the chemical composition and structure of oxides on the surface and their interaction. The material with a lower tendency to fretting corrosion will dominate in mechanical and electrochemical terms. The interaction of Ti-oxides and Co and Cr-oxides appear to depend more on the chemical composition of CoCrMo than Ti6Al4V [L. 13]. However, this requires additional testing.

The authors of [L. 13] explain the higher ΔE and E_{avg} for the Ti6Al4V-Ti6Al4V pair by the fact that the Ti6Al4V oxide layer is relatively weaker and more brittle compared to the CoCrMo oxide layer.

Figure 5 shows a comparison of changes in the coefficient of friction as a function of the duration of fretting for each test material combination.

Based on the shape of the recorded curve, it can be determined that the friction coefficient was reduced during the course of the test and then stabilized for the Ti6Al4V-Ti6Al4V and the CoCrMo-Ti6Al4V pairs, but not for the CoCrMo-CoCrMo pair. This phenomenon can be explained by the progressive

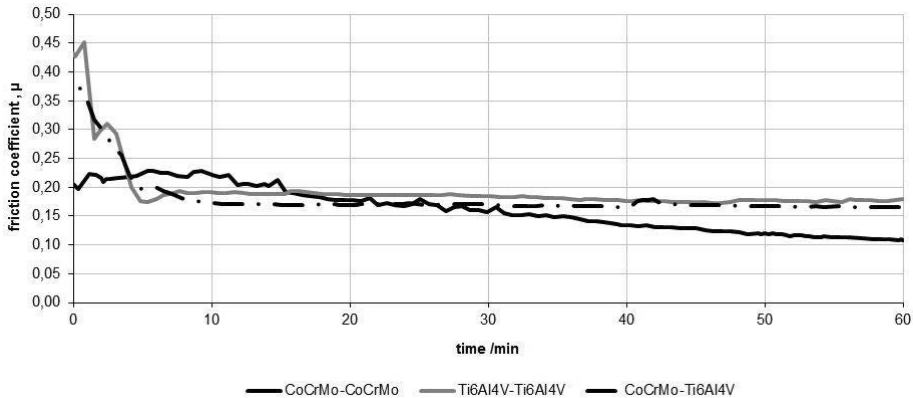


Fig. 5. Friction coefficient as function of time for different alloy combinations during the fretting phase

Rys. 5. Przebieg zmian współczynnika tarcia w funkcji czasu otrzymany dla różnych kombinacji stopów

run-in of the friction surfaces. This run-in process is particularly evident in the case of friction pairs with the participation of Ti6Al4V. In the first minutes of the fretting phase, the intense depassivation process caused by the mechanical destruction of the surface layer of the Ti-alloy was observed for the Ti6Al4V-Ti6Al4V and CoCrMo-Ti6Al4V friction pairs (**Fig. 3**). After prolonged testing time, the friction coefficient stabilized between 0.15 to 0.20 for the friction pairs with Ti6Al4V. However, for the CoCrMo-CoCrMo friction pair, the friction value is between 0.25 and 0.10, but it did not stabilise after the 3600 s of the fretting phase. A similar coefficient of friction for the tested materials was obtained by another research group [**L. 13**].

The Ti6Al4V / Ti6Al4V pair showed a slightly higher coefficient of friction. The weaker oxide layer in combination with the higher friction coefficient values between the surfaces resulted in a reduction in the corrosion resistance of the Ti6Al4V-Ti6Al4V pair [**L. 13**].

CONCLUSIONS

The analysis of the conducted testing allows us to formulate the following conclusions:

- The proposed test methodology is effective for comparison of the fretting corrosion resistance of materials used for implants.
- The CoCrMo-CoCrMo friction pair has the best corrosion resistance in bovine serum (in static conditions), while the lowest ΔE value was exhibited by the friction pair with the two dissimilar alloys, i.e. CoCrMo-Ti6Al4V.

- After the fretting phase is finished, complete reconstruction of the oxide layer does not occur within 3600 s of repassivation.
- The lowest coefficient of friction was measured for the CoCrMo-CoCrMo pair.

Acknowledgments

The research leading to these results has received funding from the European Union Seventh Framework Programme FP7/2007-2013 under grant agreement No. 602398.

Research work financed from public funds for science in period 2013–2018, granted for realization of international co-financed project.

REFERENCES

1. Jacobs J.J., Gilbert J.L., Urban R.M., Current Concepts Review, “Corrosion of Metal Orthopaedic Implants”, J Bone and Joint Surgery, 1998, 80-A(2), 268–282,
2. Wielowiejska-Giertuga A., Miler M., (3) Sulej-Chojnacka J., Badania tarciowo-zużyciowe skojarzeń materiałowych typu metal–polimer znajdujących zastosowanie w implantach ortopedycznych, Obróbka Plastyczna Metali, vol. XXVII nr 1 (2016), s. 73–82.
3. Cooper H.J., Della Valle C.J., Berger R.A., Tetreault M., Paprosky W.G., Sporer S.M., Jacobs J.J., Corrosion at the Head-Neck Taper as a Cause for Adverse Local Tissue Reactions After Total Hip Arthroplasty, J Bone Joint Surg Am, 2012, 94, 1655–61.
4. Sin J.R., Suñer S., Neville A., Emami N., Fretting corrosion of hafnium in simulated body fluids, Tribology International, 2014, 75, 10–15.
5. Billi F., Onofre E., Ebramzadeh E., Palacios T., Escudero M.L., Garcia-Alonso M.C., Characterization of modified Ti6Al4V alloy after fretting–corrosion tests using nearfield microscopy, Surface & Coatings Technology, 2012, 212, 134–144.
6. Royhmana D., Patel M., Runa M.J., Jacobs J.J., Hallab N.J., Wimmer M.A., Mathew M.T., Fretting-corrosion in hip implant modular junctions: New experimental set-up and initial outcome, Tribology International, 2015, 91, 235–245.
7. Geringer J., Macdonald D.D., Friction/fretting-corrosion mechanisms: Current trends and outlooks for implants, Materials Letters 134(2014)152–157.
8. Dąbrowski J.R., Klekotka M., Sidun J., Fretting and fretting corrosion of 316L implantation steel in the oral cavity environment, Maintenance and Reliability, 2014, 16, 3, 441–446.
9. Yan Y., Neville A., Dowson D., Tribo-corrosion properties of cobalt-based medical implant alloys in simulated biological environments, Wear 263 (2007) 1105–1111.

10. Tritschler B., Forest B., Rieu J., Fetting corrosion of material for orthopaedic implants: a study of a metal/polymer contact in an artificial physiological medium, *Tribology international* 32, 1999, 587–596.
11. Kumar S., Sankara Narayanan T.S.N., Ganesh Sundara Raman S., Seshadri S.K., 2010. Evaluation of fretting corrosion behaviour of CP-Ti for orthopaedic implant applications. *Tribology International* 43, 7, 2010, 1245–1252.
12. Bryant M., Farrar R., Frejman R., Brummitt K., Neville A., The role of surface pre-treatment on the microstructure, corrosion and fretting corrosion of cemented femoral stems, *Biotribology* 5, 2016, 1-15.
13. Swaminathan V., Gilbert J.L., Fretting corrosion of CoCrMo and Ti6Al4V interfaces, *Biomaterials* 33 (2012) 5487–5503.

Streszczenie

Najważniejszą zaletą stosowania endoprotez modułarnych stawu biodrowego jest możliwość adaptacji wymiarowej endoprotezy do osobniczych cech pacjentów. Niemniej, dodatkowa powierzchnia kontaktu narażona jest na zużycie wskutek wzajemnych mikroprzemieszczeń i agresywnego działania środowiska (korozja frettingowa).

Współcześnie stosowane endoprotezy stawu biodrowego zbudowane są z trzpienia, głowy oraz panewki (Rys. 1). Trzpień wykonany jest ze stali nierdzewnej, CoCrMo lub stopu tytanu. Głowa endoprotezy wykonana jest ze stali nierdzewnej, COCrMo lub materiału ceramicznego. W przypadku endoprotez modułarnych, gdzie połączenie modułarne znajduje się w części szyjkowej trzpienia endoprotezy, w większości stosowanymi materiałami są CoCrMo oraz Ti6Al4V.

W ramach niniejszej pracy dokonano badań porównawczych odporności na korozję frettingową trzech najczęściej spotykanych skojarzeń materiałowych występujących w połączeniach modułarnych endoprotez całkowitych stawu biodrowego (CoCrMo-CoCrMo, CoCrMo-Ti6Al4V i Ti6Al4V-Ti6Al4V). Badania przeprowadzono z zastosowaniem testera tribologicznego pracującego ślizgowo w ruchu posuwisto-zwrotnym, zintegrowanego z potencjostatem wyposażonym w układ trójelektrodowy. Skojarzenie badawcze składało się z nieruchomego trzpienia dociskanego stałą siłą do płytki wykonującej ruch posuwisto-zwrotny z zadaną częstotliwością i amplitudą. Testy przeprowadzono w środowisku roztworu wodnego surowicy bydlęcej w temperaturze 37°C.

Na podstawie uzyskanych wyników badań stwierdzono, że największą odporność korozyjną w warunkach statycznych wykazywała para trąca: CoCrMo-CoCrMo, natomiast najniższą wartość ΔE CoCrMo-Ti6Al4V. Potwierdzono także występowanie korelacji pomiędzy intensywnością procesu depasywacji spowodowanego niszczeniem mechanicznym warstwy wierzchniej a wartościami oporów tarcia w systemie tribologicznym.